Journal of the European Ceramic Society 17 (1997) 505–512

PII: S0955-2219(96)00089-1
0955-2219/97/$17.00

Growth of Indentation Cracks in Poled and Unpoled PZT

F. Guiu,[a] B. S. Hahn,[b] H. L. Lee[b] & M. J. Reece[a,*]

[a]Department of Materials, Queen Mary & Westfield College, University of London, Mile End Road, London E1 4NS, UK
[b]Department of Ceramic Engineering, Yonsei University, 134 Shinchon-dong, Sudaemoon-Ku, Seoul, 120-749, Korea

(Received 15 February 1996; revised version received 17 April 1996; accepted 3 May 1996)

Abstract

The growth behaviour of indentation cracks in both poled and unpoled PZT is examined by subjecting the cracks to static and cyclic loading in bending. An anomalous growth of the cracks not subjected to any direct stressing was observed during cyclic fatigue loading in both the poled and unpoled materials. In the poled PZT specimens the length of the radial indentation cracks was found to be strongly dependent on their orientation with respect to the poling direction, in agreement with previously reported observations. The growth behaviour of the cracks is discussed after having estimated the magnitude of their total stress intensity factor. It is argued that the apparent fracture toughness anisotropy with respect to the direction of poling is not entirely consistent with previously proposed interpretations, and an alternative explanation is suggested.

1 Introduction

Ferroelectric and piezoelectric ceramics are used in large quantities in a variety of applications in which they are not normally mechanically stressed to a significant extent. Consequently, the mechanical properties of these materials have not been of great relevance to their use and are, in fact, relatively poor. The mechanically related problems most common in ferroelectric ceramics arise from internal stresses generated by the phase changes occurring when they are cooled through the Curie temperature and from the switching and reorientation of the ferroelectric domains when they are poled. The continuous operation of these materials under alternating electrical fields, or cyclic loads, can produce a degradation of their electrical properties, and this effect can have a mechanical origin. Since they were not intended to be used as structural materials, the study of their mechanical properties has been largely neglected. As increasing demand is being placed on their performance in applications requiring very long life and large displacements under continuous operation, the interaction between their electrical and mechanical properties has become more critical and important.

Interest in the damage produced by mechanical fatigue[1,2] and the behaviour of cracks under both mechanical loads[3–5] and electric fields[6] has increased in recent years. In this paper we report the results of an investigation into the growth behaviour of cracks produced by indentation in poled and unpoled PZT when they are subjected to static and cyclic loads.

2 Material and Experimental Techniques

The material used in the present investigation was a conventional high-performance PZT (43/45) material of the following composition: $0{\cdot}12Pb(Mn_{1/3}, Sb_{2/3})O_3 - 0{\cdot}449PbTiO_3 - 0.431PbZrO_3$. Plates were prepared by cold-isostatic pressing the powders and sintering at 1200°C for 2 h. Prismatic bars (dimensions 6 × 4 × 45 mm) for four-point bending were cut from the plates using a diamond wheel. They were subsequently annealed at 600°C for 24 h to eliminate residual machining stresses and the surfaces were polished with 20 μm diamond paste. Some of the samples thus prepared were poled in a direction perpendicular to the long axis of the specimens and parallel to the 4 mm dimension with an electric field of 25 kV cm^{-1} at 100°C for 30 min. The resulting piezoelectric material was a high k_p type with $k_p = 0{\cdot}6$, $Qm = 1000$ and $E_\gamma = 900$ (measured at 30 kV cm^{-1}). After the poling stage, the small lateral faces (4 × 45 mm)

*To whom correspondence should be addressed.

of all of the specimens were further polished down to a fine finish with 0·1 μm linde alumina powder in aqueous solution.

The microstructure of the specimens was examined on polished and etched surfaces using scanning electron microscopy (SEM). The etching procedure consisted of a 10 s submersion in a mixture of 10% HCl + one drop of HF. Figure 1 shows the microstructure of a poled specimen. The average grain size is ~ 3 μm and the domain structure within the individual grains is apparent.

Vickers hardness indentations for different loads were made on the finely polished surface of the samples to measure the hardness of the material and to determine its fracture toughness from the length of the radial indentation cracks formed. Other samples were indented with loads of 73·6, 49·1 and 24·5 N placed within the inner span of the bending beam, where a state of uniform tensile stress would exist in the bend tests. The indentation of 73·6 N was placed at the centre of the beam between the 49·1 and 24·5 N indentation. One of the diagonals of the indentations was aligned parallel to the long axis of the specimen. The lengths of the cracks formed were measured and monitored for 24 h after indentation to check that they had attained equilibrium and had not grown under the influence of the residual stress field of the indentation impression. These specimens were then subjected to four-point bending under both static and cyclic loads with the indented surface in tension. The cyclic loading was of a sine waveform, frequency of 10 Hz, and with a variable load ratio P_{min}/P_{max}, but with P_{min} always kept equal to 5 N. The tests were interrupted at regular intervals and the length of the radial indentation cracks measured with an optical microscope to determine their growth. The loads were increased slowly from a small value to that necessary to initiate the growth of the indentation cracks. If the cracks stopped growing under a given applied load, or cyclic load amplitude, the load was increased by a small amount to resume their growth. This process was repeated until the specimen failed, which always occurred at the site of the largest indentation (73·6 N).

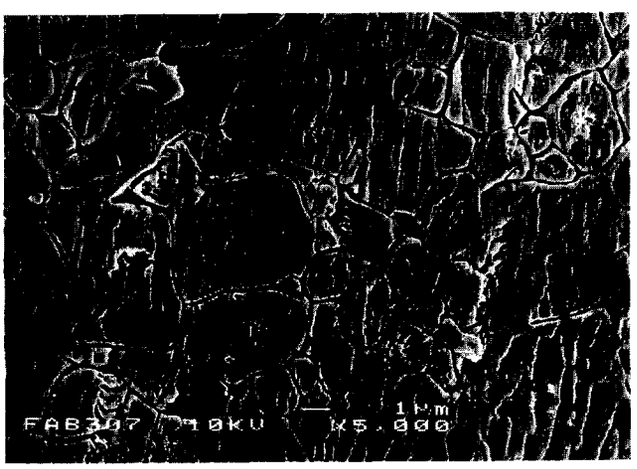

Fig. 1. Etched microstructure of the PZT material, revealing grain boundaries and ferroelectric domain structure.

3 Results

3.1 Hardness and indentation toughness

The square of the size of the half-diagonal lengths, a^2, of the indentations produced by different loads, P, is presented in Fig. 2 for both the poled and unpoled materials. The hardness H, defined as $H = P/2a^2$, can be obtained from the plots of Fig. 2, which gives values of approximately 3 GPa for both the unpoled and the poled materials.

The size of the radial cracks emanating from the corners of the indentations was greatly influenced by the poling and its direction. In the unpoled material all of the cracks had the same length. In the poled material, however, the cracks that grew in the direction normal to the poling were much longer than the cracks parallel to the poling direction. This effect has been reported before for PZT materials and has been known for some time.[4,5,7] Plots of indentation load against $c^{3/2}$, where c is the crack length, are shown in Fig. 3, where c_1 and c_2 are defined. Values of indentation fracture toughness can be obtained from these plots using the expression:[8]

$$K_{IC} = k(E/H)^{1/2}Pc^{-3/2} \quad (1)$$

where E is the Young's modulus of the material and k is a dimensionless constant that is determined experimentally and takes different values according to different authors. The fracture toughness K_{IC} estimated by the indentation method is based on the idea that the radial indentation cracks are driven to their final size by the residual

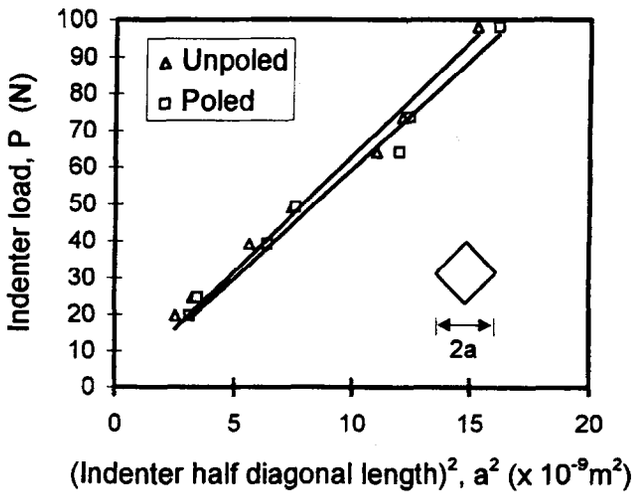

Fig. 2. Plot of indentation load against the square of the indentation half diagonal length.

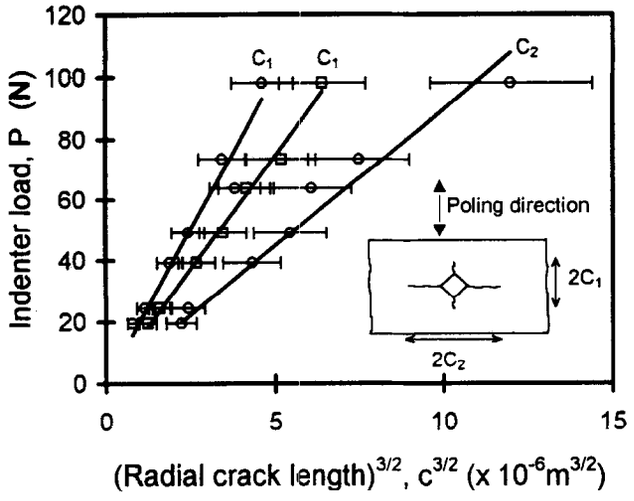

Fig. 3. Plot of indentation load against the radial crack length to the power of 3/2 used to obtain fracture toughness values. The direction of the cracks c_1 and c_2 are indicated in the inset figure. □ represent data for unpoled specimens; ○ represent data for the poled specimens.

stress field of the plastic zone associated with the indentation impression. This stress field is assumed to have radial symmetry in an isotropic material and it decreases with the distance from the centre of the indentation, so that the crack extension force, or more precisely the crack stress intensity factor K, decays as $c^{-3/2}$. The radial cracks attain an equilibrium length when this stress intensity factor reaches a value equal to the fracture toughness, K_{IC}, of the material. In the calculation of K_{IC} from eqn (1) we shall use the value of $k = 0{\cdot}016 \pm 0{\cdot}004$ given by Anstis *et al.*[8] for consistency with measurements made by others on PZT.

For an anisotropic material like PZT there is the problem of deciding which value to take for the Young's modulus, E. Pisarenko *et al.*[4] have chosen to use $1/s_{11}$ for cracks perpendicular to the poling direction and $1/s_{33}$ for cracks parallel to the poling direction, s_{ij} being the corresponding elastic compliances. While the difference between s_{11} and s_{33} is only 10 to 20% in similar PZT material,[4,9] the fact remains that there is no justification for adopting this procedure and we have opted for measuring directly and experimentally the ratio E/H by the Knoop indentation method proposed by Marshall *et al.*[10]

Several Knoop indentations were made with different loads ranging between 24·5 and 98·1 N on the surface of both unpoled and poled specimens, with the long diagonal of the indentation aligned both parallel and perpendicular to the poling direction. The length of the diagonals was found to be independent of the orientation of the impression and have a constant ratio, $b'/a' = 0{\cdot}27$, within the experimental measuring error, for all the different indentation loads used and for both poled and unpoled material. Using the data of Ref. 10 a value of $H/E = 0{\cdot}034$ was obtained with this technique, so that eqn (1) is simplified to

$$K_{IC} = 0{\cdot}08\frac{P}{c^{3/2}} \tag{2}$$

and from the slope of the plots of Fig. 3 we obtain:

$$K_{IC} = 1{\cdot}2 \pm 0{\cdot}1 \text{ MPa m}^{1/2}$$

for the unpoled PZT

$$K_{IC} = 1{\cdot}6 \pm 0{\cdot}3 \text{ MPa m}^{1/2}$$

for the poled PZT, cracks parallel to poling direction

$$K_{IC} = 0{\cdot}7 \pm 0{\cdot}1 \text{ MPa m}^{1/2}$$

for the poled PZT, cracks normal to poling direction

These values are similar to those given by other authors for similar materials,[4,5,7] but allowance has to be made for some error in the absolute values of the fracture toughness usually quoted due to uncertainties in the value of the coefficient k and the ratio E/H in eqn (1).

An important aspect of the results is the crack length anisotropy in the poled PZT. Some authors have explained this effect as being due to the anisotropy in the internal stresses induced by poling.[7] This explanation has been challenged by other researchers, who attributed the effect to a real toughness anisotropy.[4,5] This would arise, it is argued, from the stress-induced switching, or reorientation, of the 90° ferroelectric domains which can occur at the tip of cracks growing in a plane parallel to the poling direction but not at the tip of cracks growing in a plane normal to the poling direction. Both these interpretations attempt to explain the difference in indentation crack lengths in poled PZT and the toughness anisotropy, or values of K_{IC}, resulting thereof when they are calculated by the standard indentation methods developed for isotropic materials. It is in this context interesting to note that measurements of stable crack growth rates made in a similar PZT material did not reveal the same anisotropy, but rather the opposite effect.[3] When subjected to the same applied stress intensity factor in a double torsion test, cracks in a plane parallel to the poling direction grew at a faster rate than cracks in a plane perpendicular to the direction of poling. Also, in a more recent publication, Mehta and Virkar[5] report measurements of fracture toughness for (0·54/0·56) PZT measured by the single edge notched bend method which produced values of $K_{IC} = \sim 0{\cdot}98$ MPa m$^{1/2}$ for samples poled along the notch surface and $K_{IC} = \sim 1{\cdot}2$ MPa m$^{1/2}$ for samples poled in a direction perpendicular to the notch surface. The fracture toughness of unpoled samples, was, however, $K_{IC} = \sim 1{\cdot}45$ MPa m$^{1/2}$. These results reveal a higher toughness for the unpoled material and hardly any anisotropy for

the poled samples, something which is not consistent with the measurement of K_{IC} by indentation, but is, however, consistent with the results of static crack growth referred to above.[3] Pisarenko *et al.*[4] reported similar discrepancies in the values of fracture toughness anisotropy obtained using different methods of measurement.

In the light of these discrepancies, perhaps one should consider the possibility that the observed anisotropy in the indentation crack lengths for the poled material could arise also from an anisotropy, or asymmetry, in the residual stress field generated by the indentation. We shall return to this point later.

3.2 Stable growth of cracks subjected to cyclic and static loading

The growth behaviour of the indentation cracks when they are subjected, in four-point bending, to both static and cyclic tensile stresses is displayed in Figs 4 to 7. The total length $2c$ of the radial cracks is plotted against number of fatigue cycles or time. The static bending loads or peak loads amplitudes applied during the tests are also indicated in the figures. With the dimensions of the specimens used in the experiments, the relation between the load and the maximum tensile stress, on the tensile surface of the specimens, is simply given by $\sigma = P/4{\cdot}8$, where P is the bending load in N and σ is stress in MPa. For example, a 100 N applied load corresponded to a maximum tensile stress of 20·8 MPa.

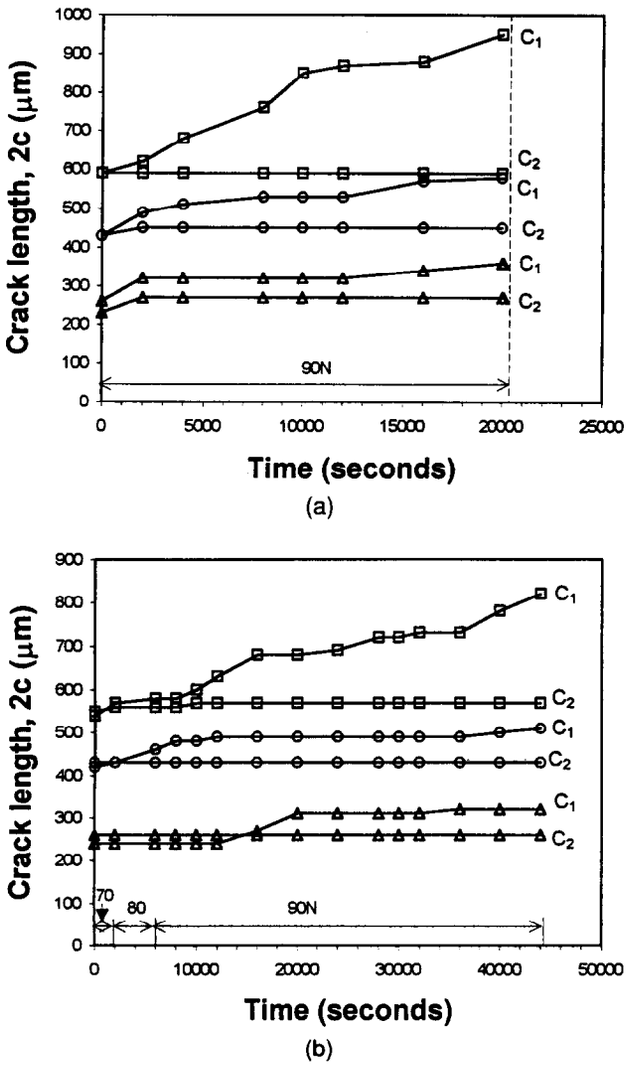

Fig. 4. (a) and (b) Plots of crack length against time in unpoled specimens statically stressed with a sequence of static loads as shown in the figure. The crack directions c_1 and c_2 are as defined in Fig. 3. Radial cracks from: □, 73·6 N indentations; ○, 49·1 N indentations; △, 24·5 N indentations.

3.2.1 Results for the unpoled specimens

It is immediately apparent that in the unpoled samples the cracks statically stressed (Fig. 4) grew at a faster rate than those subjected to cyclic stresses (Fig. 5) of the same maximum stress. The cracks in the statically loaded specimens grew progressively under constant applied load. However, the cracks in the cyclically loaded specimens required the application of an increasing load amplitude in order to maintain their growth.

While the cracks parallel to the axis of the bending beam were not subjected to any directly applied stress, their length was observed to grow over a small distance during the first 10000 s following the load application before finally becoming arrested. This effect is particularly prominent in the cyclic fatigue loading mode when the total crack length, $2c$, increased by as much as 100 μm.

3.2.2 Results for the poled specimens

The crack growth results for the poled samples are shown in Figs 6 and 7, where the loading sequences used in the tests are also shown. The anisotropy in the initial length of the indentation cracks with respect to the direction of poling is clearly apparent. Again, it should be noted that the growth rate of the statically stressed cracks

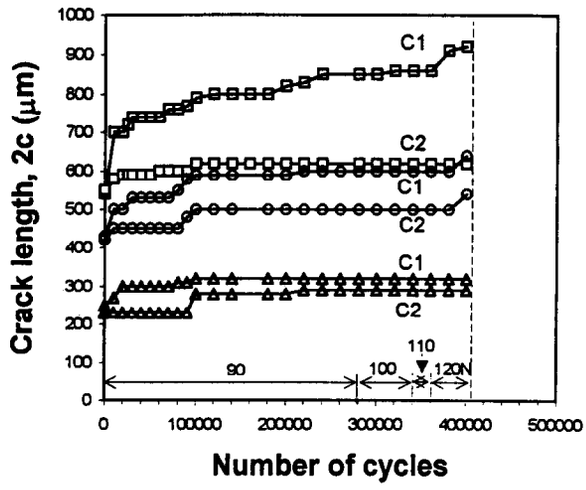

Fig. 5. Plots of crack length against the number of cycles in unpoled specimens cyclically loaded with the peak load sequences shown in the figure. The symbols have the same meaning as in Fig. 4.

(Fig. 6) was greater than that of the cyclically loaded cracks (Fig. 7) when they were subjected to similar loading sequences. The anomalous growth

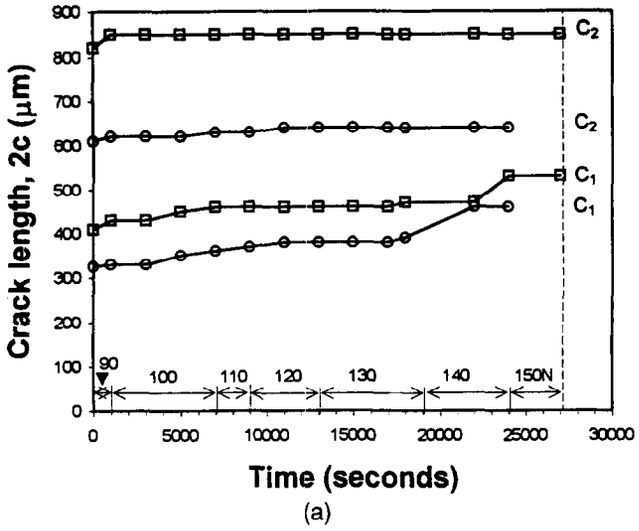

(a)

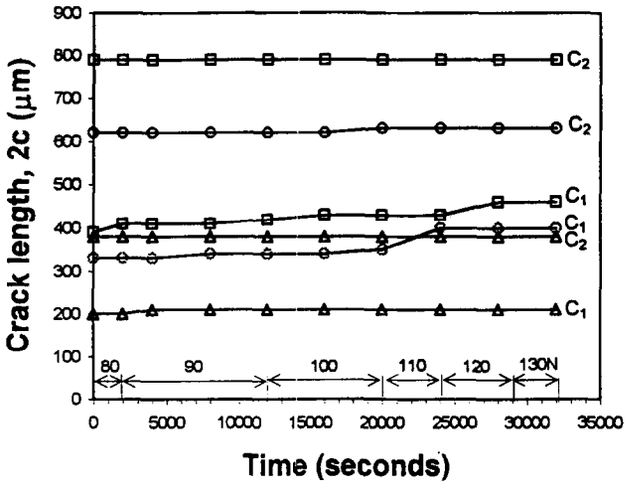

(b)

Fig. 6. (a) and (b) Plots of crack length against time in poled bend specimens statically loaded with the sequence of loads shown in the figure. The symbols have the same meaning as in Fig. 5.

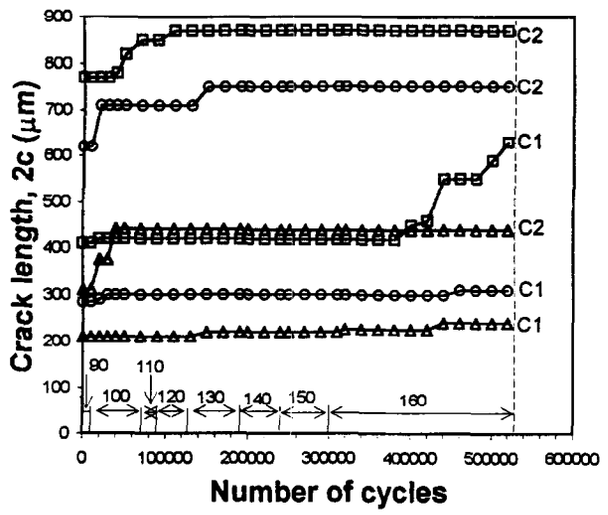

Fig. 7. Plots of crack length against the number of cycles in poled specimens cyclically loaded with the peak load sequences shown in the figure. The symbols have the same meaning as in Fig. 5.

of the unstressed long cracks, c_2, parallel to the specimen length was also observed, particularly in the cyclically stressed specimens, where the radial cracks from the 49·1 N indentations grew by as much as 130 μm.

It is worth noting that the short cracks, c_1, parallel to the poling direction from the 73·6 N indentations did not grow in cyclic fatigue until the load had been increased to 160 N, and that those from the 49·1 N indentations had only grown by a relatively small amount (~25 μm) by the end of the test. A similar, but smaller, resistance to the growth of the short cracks could be detected in the static load tests.

4 Discussion

In order to understand and discuss the behaviour of the radial indentation cracks, it is helpful to have an estimate of the values of the stress intensity factor acting on them during their growth. The stress intensity factor arising from the applied bending load can be obtained from the Raju–Newman solution for a semi-elliptical surface crack:[11]

$$K_a = \frac{C\sigma(\pi c)^{1/2}}{\Phi} \tag{3}$$

where the constants C and Φ depend on crack length, specimen size and the eccentricity of the elliptical crack. For a semi-circular crack and the dimensions of the specimens used in our tests, eqn (3) reduces to:

$$K_a = 1{\cdot}144(2/\pi)\sigma(\pi c)^{1/2} = 1{\cdot}29\sigma c^{1/2} \tag{4}$$

The cracks were also subjected to the residual stress intensity factor K_r resulting from the indentation stress field, which decreases as the crack length increases. The values of K_a, K_r and the total stress intensity factor, $K_t = K_a + K_r$, are plotted against time in Figs 8 to 12 for the 73·6 and 49·1 N indentations for both poled and unpoled specimens and for the different loading conditions.

4.1 Unpoled specimens

The cracks in the unpoled specimens, subject to two different sequences of static loading, grew in a stable manner with a continuously decreasing stress intensity factor, K_t (Fig. 8). This is the anticipated behaviour for stable growth of the cracks. The crack instability, corresponding to specimen failure, should occur when the rate of change of K_t with crack length changes from negative to positive. This is not inconsistent with the results plotted in Figs 8(a) and 8(b) which show very similar trends and where it can be seen that the critical value of K_t at which failure occurred coincides

with the value of fracture toughness, K_{IC}, measured by the indentation method.

Very similar and consistent results were obtained for the growth of cracks under cyclic loading. It can be seen in Fig. 9 that the crack from a 73·6 N indentation grew in a stable manner under a decreasing K_t and became unstable after K_t had reached a minimum value and started increasing. The critical value of K_t at fracture was, again, nearly the same as the fracture toughness K_{IC} measured by the indentation method. It appears from these results and observations that the unpoled material behaved as one would expect for a monolithic ceramic. A similar behaviour was also found for the cracks of a 49·1 N indentation in the same specimen (Fig. 10).

The growth of the indentation cracks c_2, not subjected to any directly applied stress, is a more unusual result which is more prominent in cyclic loading. These cracks must have reached an equilibrium length in the indentation residual stress field at indentation unloading. They were then able to grow during the early stages of the cyclic tests by a small amount with no additional direct stress and under an apparently decreasing stress intensity factor, K_r (Figs 9 and 10). Similar, unexplained, observations regarding the anomalous extension of longitudinal unstressed cracks have been reported by White *et al.*[1] during the cyclic loading of PZT bars driven at their resonant frequency of 24 kHz and at a temperature of ~200°C. We do not know of any similar results having been reported for any other ceramic and this suggests that the effect is peculiar to the ferroelectric nature of PZT. It is possible that, assisted by the cyclic tensile stress parallel to the crack faces, switching of the 90° domains near the free crack surfaces may have occurred[5] causing fluctuations in the residual stress field of the cracks, or producing mismatch of the crack faces capable of exciting a fatigue crack growth mechanism.[12] Following this interpretation, these cracks would become permanently arrested when K_r had

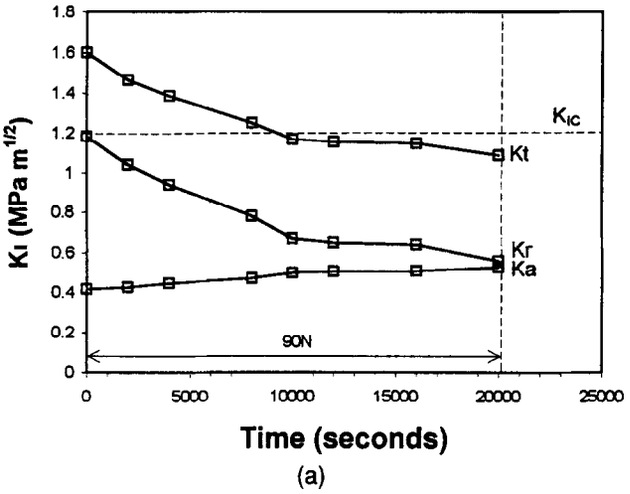

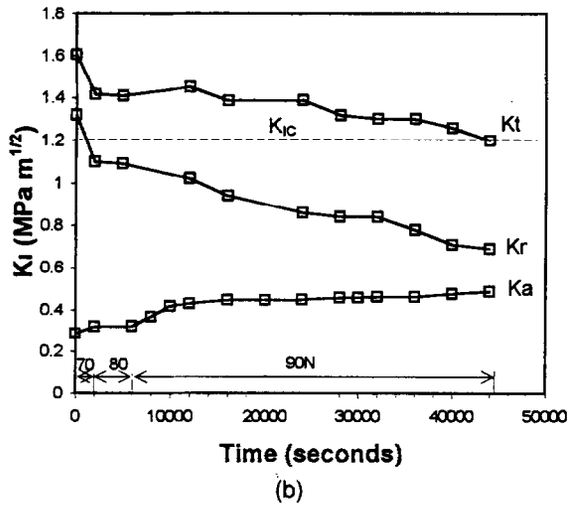

Fig. 8. (a) and (b) Plots of residual stress intensity factor K_r, applied stress intensity factor K_a and total stress intensity factor K_t acting on the cracks in the unpoled statically loaded specimens of Fig. 4.

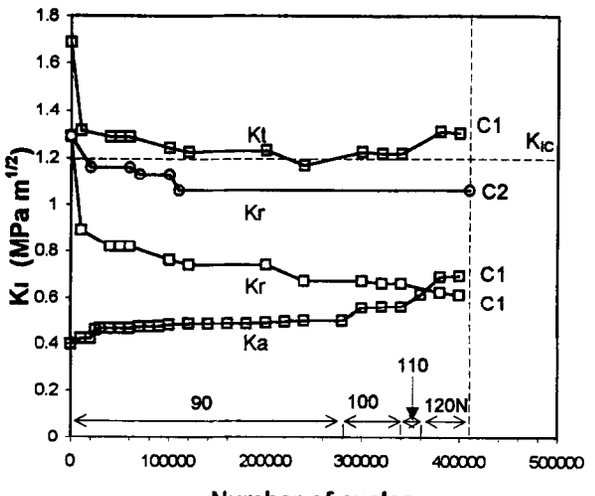

Fig. 9. Plot of K_r, K_a and K_t acting on the 73·6 N indentation cracks c_1 and c_2 of the unpoled cyclically loaded specimen of Fig. 5.

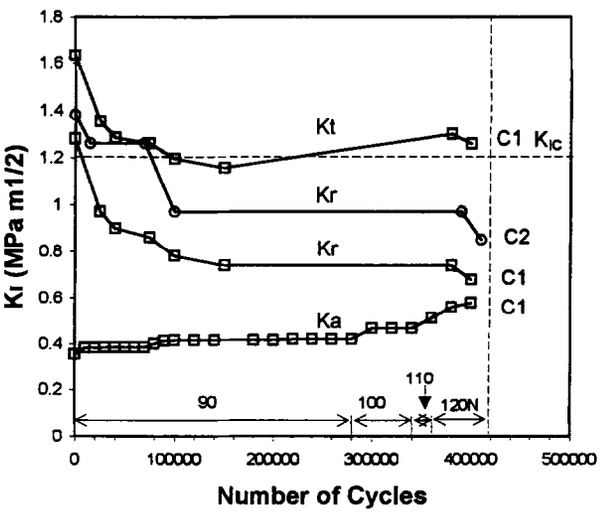

Fig. 10. Plot of K_r, K_a and K_t acting on the 49·1 N indentation cracks c_1 and c_2 of the unpoled cyclically loaded specimen of Fig. 5.

decreased to a threshold value insufficient to provide the necessary driving force. From the data of Figs 9 and 10, it appears that this threshold value was between 0·8 and 1·1 MPa $m^{1/2}$.

4.2 Poled specimens

The most remarkable observation for the poled specimens is that the cracks c_1, parallel to the poling direction, grew at a much slower rate than in the unpoled samples even though they were subjected to a total stress intensity factor which remained fairly constant at approximately 2·1 MPa $m^{1/2}$ for the statically loaded specimens [Figs 11(a) and (b)] and had to be increased well above this value before the cracks started growing in the cyclically loaded specimens (Fig. 12). This behaviour is difficult to understand even if one accepts the previously suggested view that the material has a higher fracture toughness in the direction parallel to the poling direction. This proposition would not explain why indentation cracks which had reached equilibrium under a residual stress intensity factor K_r of approximately 1·9 MPa $m^{1/2}$ would not grow until the total stress intensity factor K_t was increased by the applied stress to 2·4 MPa $m^{1/2}$. Note, however, that the cracks c_2 in a plane normal to the poling direction, which were unstressed, grew by a small distance to a final equilibrium length, as they did also in the unpoled samples.

The apparent large growth resistance of the short radial cracks could be understood if the residual stress intensity factor K_r acting on those cracks was smaller than has been supposed. A smaller value of K_r than that obtained by using eqn (2) would be possible if the presence of the crack itself had relaxed the indentation residual stress through domain switching made possible by the presence of the crack free surfaces.[5] Another possibility, for which there is no evidence as yet, is that the residual stress field produced beneath the indentation in the poled PZT is anisotropic, having higher intensity, or being longer range, in the direction normal to poling. The implicit assumption that the fracture toughness, or K_r, of an anisotropic poled PZT material can be obtained using eqn (2) perhaps needs careful examination. Although the elastic anisotropy of poled PZT, measured by the ratio s_{11}/s_{33}, is only about 0·8,[4,9] the anisotropy of an indentation residual stress field could be much greater than this because it arises from the plastic deformation of the material beneath the indentation and the plastic deformation field itself could be anisotropic. The anisotropy in the plastic deformation field can be induced by the preferred orientation of the ferroelectric domains in the polarized material and differences in the shear moduli c_{44} and c_{66}. To our knowledge this possibility has never been addressed but it is attractive because it would explain, in a very simple manner, some of the discrepancies

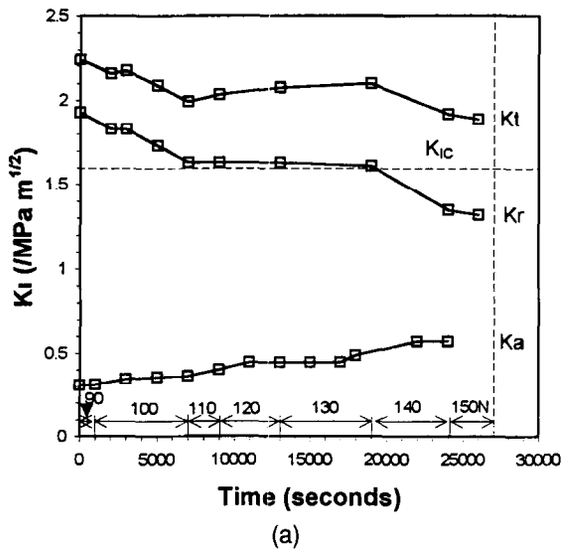

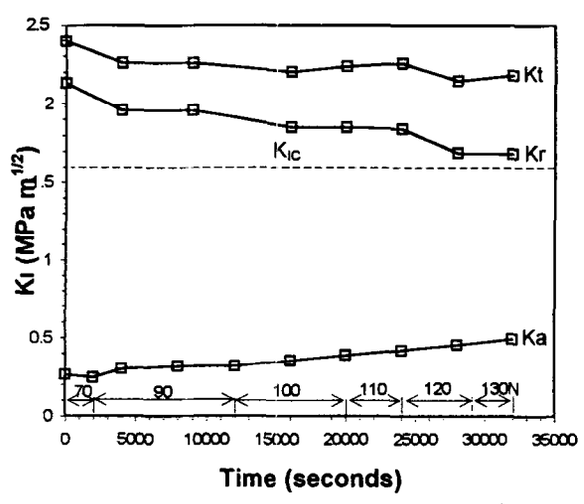

Fig. 11. (a) and (b) Plot of K_r, K_a and K_t acting on the 73·6 N indentation cracks of the poled statically loaded specimen of Fig. 6.

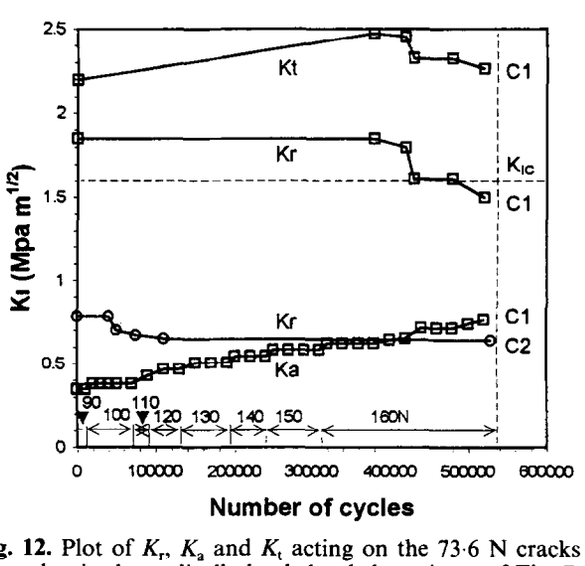

Fig. 12. Plot of K_r, K_a and K_t acting on the 73·6 N cracks c_1 and c_2 in the cyclically loaded poled specimen of Fig. 7.

already mentioned above, namely that the fracture toughness anisotropy measured by the indentation method [between 2·3 and 3·5 (Refs 4, 5 and present work)] is much greater than when it is measured by other methods (between 0·9 and 1·2[4,5]).

Acknowledgements

Professor Hong Lim Lee's sabbatical leave at Queen Mary & Westfield College was supported by The Center for Interface Science and Engineering Materials, South Korea. We would also like to thank The British Council for their support under the Acciones Integradas Programme and Dr Basilio Jimenez Diaz at Instituto de Ciencia de Materiales de Madrid for his comments during the work.

References

1. White, G. S., Raynes, A. S., Vaudin, M. D. & Freiman, S. W., Fracture behaviour of cyclically loaded PZT. *J. Am. Ceram. Soc.*, **77** (1994) 2603.
2. Lynch, C. S., Chen, L., Suo, Z., McMeeking, R. M. & Yang, W., Crack growth in ferroelectric ceramics driven by cyclic polarization switching. *J. Intell. Mater. Systems Struct.*, **6** (1995) 191.
3. Bruce, J. G., Garberich, W. W. & Koepke, B. G., Subcritical crack growth in PZT. In *Fracture Mechanics of Ceramics, Vol. 5*, eds D. P. H. Hasselman & F. F. Lange. Plenum, New York, 1978, p. 687.
4. Pisarenko, G. G., Chushko, V. M. & Kovalev, S. P., Anisotropy of fracture toughness of piezoelectric ceramics. *J. Am. Ceram. Soc.*, **68** (1985) 259.
5. Mehta, K. & Virkar, A., Fracture mechanisms in ferroelectric–ferroelastic lead zirconate titanate (Zr:T = 0·54 : 0·46) ceramics. *J. Am. Ceram. Soc.*, **73** (1990) 56.
6. Cao, H. & Evans, A. G., Electric-field-induced fatigue crack growth in piezoelectrics. *J. Am. Ceram. Soc.*, **77** (1994) 1783.
7. Yamamoto, T., Igarishi, H. & Okazaki, K., Mechanical properties of (Pb, Ca) TiO_3 family ceramics with zero planar coupling factor. *Ceram. Int.*, **11** (1985) 75.
8. Anstis, G. R., Chantikul, P., Lawn, B. R. & Marshall, D. B., A critical evaluation of indentation techniques for measuring toughness, I, Direct crack measurements. *J. Am. Ceram. Soc.*, **64** (1981) 533.
9. Catalogue of 'Piezoelectric Ceramic Products', Morgan Matroc Ltd, Unilator Division, UK.
10. Marshall, D. B., Noma, T. & Evans, A. G., A simple method for determining elastic-modulus-to-hardness ratios using Knoop indentation measurements. *J. Am. Ceram. Soc.*, **65** (1982) C177–C176.
11. Raju, I. S. & Newman, J. C. Jr, Stress intensity factors for a wide range of semi-elliptical cracks in finite thickness plates. *Eng. Fract. Mech.*, **11**, (1979) 817.
12. Reece, M. J., Vaughan, D. & Guiu, F., Cyclic fatigue of ceramics. *J. Mater. Sci.*, **26** (1991) 3275.